THE CANADIAN MINERALOGIST

Journal of the Mineralogical Association of Canada

Volume 17 February 1979 Number 1

Canadian Mineralogist
Vol. 17, pp. 1-10 (1979)

THE CRYSTAL CHEMISTRY OF THE AMPHIBOLES. X. REFINEMENT OF THE CRYSTAL STRUCTURE OF FERROGLAUCOPHANE AND AN IDEAL POLYHEDRAL MODEL FOR CLINOAMPHIBOLES

F. C. HAWTHORNE

Department of Earth Sciences, University of Manitoba, Winnipeg, Manitoba R3T 2N2

ABSTRACT

Three-dimensional counter-collected single-crystal X-ray data and a full-matrix least-squares method were used to refine the crystal structure and cation-ordering pattern of a ferroglaucophane [a 9.587(4), b 17.832(7), c 5.315(2)Å, β 103.47(3)°; $C2/m$] from Calabria, Italy. The final R index for 1015 observed reflections is 3.2%. The cation-ordering pattern in ferroglaucophane is similar to that exhibited by glaucophane (Papike & Clark 1968). The site-population refinement for ferroglaucophane indicates a small amount of Al in M(1), or M(3), or both; mean-bond-length considerations suggest that this Al is strongly ordered in M(1). An ideal geometrical model is presented for the clinoamphiboles, similar to the models presented by Thompson (1970) and Papike & Ross (1970), but involving extended rather than rotated tetrahedral chains. In this ideal structure, the atomic coordinates closely resemble those of grunerite (Finger 1969c); the articulation requirements indicate that the tetrahedral chain rotation is a function of the ratio of two mean bond lengths (octahedral m.b.l./tetrahedral m.b.l., allowing for various perturbations due to cation–cation repulsion and cation ordering. Bond-strength requirements in the neighborhood of M(4) suggest that tetrahedral rotations must be O rotations, as S rotations would contribute excess bond strength to O(6).

SOMMAIRE

On a affiné la structure et la mise en ordre des cations d'un ferroglaucophane de Calabre (Italie) sur cristal unique [a 9.587(4), b 17.832(7), c 5.315(2)Å, β 103.47(3)°; $C2/m$], à partir de données tridimensionnelles recueillies sur diffractomètre à compteur (1015 réflexions observées), par la méthode des moindres carrés à matrice complète, jusqu'au résidu R = 0.032. L'ordonnance des cations ressemble à celle que montre le glaucophane (Papike & Clark 1968). L'affinement du ferroglaucophane indique une faible quantité d'Al en M(1), en M(2), ou en M(1) et M(2) à la fois; les longueurs moyennes de liaison font penser que Al est fortement ordonné en M(1). On présente un modèle géométrique idéalisé des clinoamphiboles, semblable aux modèles de Thompson (1970) et de Papike & Ross (1970), mais qui met en oeuvre l'extension plutôt que la rotation des chaînes de tétraèdres. Dans ce modèle, les coordonnées atomiques sont très proches de celles de la grunerite (Finger 1969c), et les exigences d'articulation montrent que la rotation des chaînes de tétraèdres est fonction du rapport entre deux longueurs moyennes de liaison (celle de l'octaèdre et celle du tétraèdre), compte tenu des perturbations dues à la répulsion des cations entre eux et à leur mise en ordre. Les exigences des forces de liaison au voisinage de M(4) semblent impliquer des rotations de tétraèdre du type O, car des rotations S contribueraient à fournir à O(6) un excédent d'unités de valence.

(Traduit par la Rédaction)

INTRODUCTION

Glaucophane is a bluish grey amphibole with an ideal formula $Na_2(Mg,Fe^{2+})_3Al_2Si_8O_{22}(OH)_2$. Its parageneses are virtually confined to blueschist-facies rocks (Ernst 1968, 1973) thought to have been generated under high pressure–low temperature conditions (Ernst 1971, Coleman 1972). In most glaucophanes, there is some replacement of Al by Fe^{3+}, and complete solid solution apparently exists between glaucophane and magnesioriebeckite. Until recently, natural occurrences of amphiboles in the compositional field of ferroglaucophane were not known. However, Black (1970), Hoffmann (1970), Bocquet (1974) and Makanjuola & Howie (1972) have reported analyses of ferroglaucophane, and Hoffmann (1972) has synthesized the ferroglaucophane end-member and investigated its stability relations.

In this study, the structure of a natural ferroglaucophane has been refined in order to characterize the cation ordering pattern in the structure and to provide precise interatomic distances.

EXPERIMENTAL

The crystals used in this investigation were kindly supplied by Dr. Christoph Hoffmann, University of Gottingen. Details of the occurrence, chemistry and stability are given by Hoffmann (1970, 1972). Single-crystal precession photographs exhibit monoclinic symmetry with systematic absences *hkl*, $h+k=2n+1$, consistent with the space groups $C2/m$, $C2$ and Cm; in agreement with previous work on glaucophane (Papike & Clark 1968), the space group $C2/m$ was assumed and found to be satisfactory. Cell dimensions were determined by least-squares refinement of 15 reflections aligned automatically on a 4-circle diffractometer; the values obtained are given in Table 1 together with other information pertinent to data collection, reduction and refinement. These values were confirmed on two other crystals by the same method.

TABLE 1. MISCELLANEOUS INFORMATION

Chemical Analysis*		Unit Cell Contents**		X-ray data	
SiO_2	54.63	Si	7.94	a(Å)	9.587(4)Å
Al_2O_3	11.02	Al^{IV}	0.06	b(Å)	17.832(7)
TiO_2	0.06	Tetrahedral	8.00	c(Å)	5.315(2)
Fe_2O_3	2.76	Al^{IV}	1.83	(°)	103.47(3)°
FeO	16.02	Ti	0.01	V(Å^3)	883.64
MnO	0.08	Fe^{3+}	0.31	Sp.Gr.	C2/m
MgO	4.75	Fe^{2+}	1.94	Z	2
CaO	0.98	Mn	0.01	D_{calc}	3.224
Na_2O	6.25	Mg	1.03	μ (cm^{-1})	27.3
K_2O	0.01	Octahedral	5.13	Rad./Mono.	Mo/C
	97.56	Ca	0.15	No. of $\lvert F_{obs} \rvert$	1257
		Na	1.75	No. of $\lvert F_{obs} \rvert > 3\sigma$	1015
			1.90	Final R(obs.)	3.2%
				Final R_w(obs.)	3.4%
				Final R (all data)	4.5%
				Final R_w(all data)	4.4%

$$R=\Sigma(|F_{obs}|-|F_{calc}|)/\Sigma|F_{obs}|$$

$$R_w=\left[\Sigma w(|F_{obs}|-|F_{calc}|)^2/\Sigma wF^2_{obs}\right]^{1/2},w=1$$

Temperature factor form used: $\exp.\left[-\sum_{i=1}^{3}\sum_{j=1}^{3} h_i h_j \beta_{ij}\right]$

---

*from Hoffman (1972); **calculated on the basis of 23 oxygens p.f.u.

A single crystal measuring 0.12 x 0.10 x 0.09mm was used to collect the intensity data. The crystal was mounted on a Syntex $P2_1$ automatic 4-circle diffractometer operating in the θ–2θ scan mode with the scan rate varying between 2° and 24°/min depending on the peak count and the α_1–α_2 separation, using graphite monochromatized Mo$K\alpha$ radiation ($\lambda =$ 0.71069Å). Two standard reflections were measured every 20 reflections to check for constancy of crystal alignment; no significant change was observed during data collection. A total of 1267 reflections were measured over one asymmetric unit out to a 2θ value of 60°. The data were corrected for absorption, Lorentz, polarization and background effects, and reduced to structure factors. A reflection was considered observed if its intensity exceeds that of three standard deviations based on counting statistics. This resulted in 1257 unique reflections of which 1015 were considered as observed.

REFINEMENT

Scattering factors for neutral atoms were taken from Cromer & Mann (1968), with anomalous dispersion corrections from Cromer & Liberman (1970). The atomic parameters of glaucophane (Papike & Clark 1968) were used as input to the least-squares program RFINE (Finger 1969a). Quoted *R* indices and anisotropic temperature factors are of the form given in Table 1.

Initial site-occupancies were assigned by analogy with those of glaucophane (Papike & Clark 1968). All Al was assigned to $M(2)$, Na and Ca were assigned to $M(4)$, and Mg and Fe were assumed to be equally distributed between $M(1)$ and $M(3)$; the small amounts of $M(2)$ and $M(4)$ not occupied by Al, Na and Ca were assumed to be occupied by Fe. The atomic populations of the $M(1)$ and $M(3)$ sites were assigned as variable with their bulk chemistry constrained to the initial value (Finger 1969b). Several cycles of refinement, gradually increasing the number of variables, resulted in convergence at an *R* index of 3.8% for isotropic temperature factors. Temperature factors were converted to an anisotropic form as given in Table 1, and several cycles of least-squares refinement, gradually increasing the number of variables, resulted in convergence at an *R* of 3.5%. At this stage, the equivalent isotropic temperature factor of the $M(2)$ site was significantly less than those of $M(1)$ and $M(3)$. Examination of the octahedral-site temperature factors in ordered amphiboles (Papike *et al.* 1969, Hawthorne & Grundy 1976) indicates that they are generally equal, and this has also been confirmed for disordered and partly ordered amphiboles (Finger 1969c, Hawthorne 1976, Hawthorne & Grundy 1973a). This suggested that the scattering power at the $M(2)$ position was not correct. Thus the Fe distribution was refined over all four M sites with the bulk composition constrained to be equal to that indicated by the chemical analysis. This reduced the R factor to 3.3% and the octahedral equivalent isotropic temperature factors became equal. However, the Mg occupancy of the $M(2)$ site became negative, with the $M(2)$ Fe occupancy equal to 0.152(6); this is exactly equal to the amount of Fe^{3+} from the chemical analysis. These factors suggest that this effect is real, and that either there is a small amount of Al occurring in the $M(1)$ and $M(3)$ sites or that the amount of octahedral Al indicated by the analysis is slightly too large. As the scattering factors of Mg and Al are virtually identical, the negative $M(2)$ Mg occupancy corresponds directly to a reduction in the amount of octahedral Al in $M(2)$. The $M(2)$ position was modified so as to be occupied by Al and Fe only, and the distribution of Fe over the four M sites was refined with a bulk compositional constraint, together with all other variables. Convergence was obtained at R and R_w indices (observed data) of 3.2% respectively. Final atomic positions and equivalent isotropic temperature factors are given in Table 2 and anisotropic temperature factor coefficients are given in Table 3. Interatomic distances and angles, and the magnitudes and orientations of the principal axes of the thermal ellipsoids were calculated with the program ERRORS (L. W. Finger, pers. comm.) and are presented in Tables 4-7. Structure factor tables may be obtained at nominal cost from the Depository of Unpublished Data, CISTI, National Research Council of Canada, Ottawa, Ontario K1A 0S2.

TABLE 2. ATOMIC PARAMETERS FOR FERROGLAUCOPHANE

Atom	x	y	z	$B_{equiv.}$
O(1)	0.1089(3)	0.0947(1)	0.2016(5)	0.65(4)
O(2)	0.1178(3)	0.1730(1)	0.7478(4)	0.59(4)
O(3)	0.1129(4)	0	0.7077(7)	0.85(5)
O(4)	0.3695(3)	0.2520(1)	0.8064(5)	0.69(4)
O(5)	0.3550(3)	0.1307(1)	0.0884(5)	0.74(4)
O(6)	0.3398(3)	0.1224(1)	0.5793(5)	0.75(4)
O(7)	0.3288(4)	0	0.3022(7)	0.86(5)
T(1)	0.2824(1)	0.08732(5)	0.2922(2)	0.45(1)
T(2)	0.2926(1)	0.17268(5)	0.8079(2)	0.45(1)
M(1)	0	0.09176(7)	1/2	0.60(2)
M(2)	0	0.18168(7)	0	0.58(3)
M(3)	0	0	0	0.61(3)
M(4)	0	0.2772(1)	1/2	1.27(5)

TABLE 3. ANISOTROPIC TEMPERATURE FACTOR COEFFICIENTS* FOR FERROGLAUCOPHANE

Atom	β_{11}	β_{22}	β_{33}	β_{12}	β_{13}	β_{23}
O(1)	167(25)	58(7)	552(82)	-9(11)	14(37)	8(20)
O(2)	183(25)	53(7)	425(76)	-6(11)	61(35)	-5(19)
O(3)	276(40)	65(11)	700(124)	0	98(58)	0
O(4)	254(26)	46(7)	581(81)	-22(11)	131(39)	-13(20)
O(5)	193(26)	73(8)	580(77)	-15(11)	79(37)	66(20)
O(6)	223(26)	75(8)	472(77)	14(11)	53(38)	-63(20)
O(7)	302(41)	39(9)	902(126)	0	59(61)	0
T(1)	169(10)	34(3)	308(28)	1(4)	43(13)	3(7)
T(2)	157(9)	35(3)	323(28)	-7(4)	45(13)	-2(7)
M(1)	230(11)	45(3)	413(34)	0	92(14)	0
M(2)	185(15)	42(4)	505(46)	0	63(19)	0
M(3)	253(14)	34(4)	479(43)	0	62(18)	0
M(4)	488(29)	83(7)	1219(87)	0	402(37)	0

* $\beta_{ij} = \beta_{ij} \times 10^5$

DISCUSSION

The results of the site-population refinement are given in Table 8. The refined $M(2)$ occupancy of 0.152(6) Fe° indicates that 0.134Al

TABLE 4. SELECTED INTERATOMIC DISTANCES FOR FERROGLAUCOPHANE

Atoms	*	length (Å)	Atoms	*	length (Å)
T(1)-O(1)	1	1.625(3)	T(2)-O(2)	1	1.631(3)
T(1)-O(5)	1	1.615(3)	T(2)-O(4)	1	1.596(3)
T(1)-O(6)	1	1.623(3)	T(2)-O(5)	1	1.651(3)
T(1)-O(7)	1	1.617(1)	T(2)-O(6)	1	1.655(3)
Mean		1.620	Mean		1.633
M(1)-O(1)	2	2.093(2)	M(3)-O(1)	4	2.138(2)
M(1)-O(2)	2	2.101(2)	M(3)-O(3)	2	2.090(4)
M(1)-O(3)	2	2.124(2)	Mean		2.122
Mean		2.106	M(4)-O(2)	2	2.403(3)
M(2)-O(1)	2	2.030(3)	M(4)-O(4)	2	2.332(3)
M(2)-O(2)	2	1.950(2)	M(4)-O(5)	2	2.828(3)
M(2)-O(4)	2	1.850(3)	M(4)-O(6)	2	2.457(3)
Mean		1.943	Mean 6		2.397
A-O(5)	4	2.809(3)	Mean 8		2.505
A-O(6)	4	3.244(3)			
A-O(7)	2	2.549(4)	M(1)-M(1)	1	3.272(2)
A-O(7)	2	3.690(4)	M(1)-M(2)	2	3.104(1)
Mean 12		3.058	M(1)-M(3)	2	3.121(1)
			M(1)-M(4)	1	3.307(2)
Mean 10		2.931	M(2)-M(3)	1	3.240(1)
			M(2)-M(4)	2	3.157(1)

*bond multiplicity

TABLE 5. POLYHEDRAL EDGE LENGTHS (Å) FOR FERROGLAUCOPHANE

Atoms	*	Distance
T(1) tetrahedron		
0(1)-0(5)	1	2.646(3)
0(1)-0(6)	1	2.665(3)
0(1)-0(7)	1	2.657(4)
0(5)-0(6)	1	2.651(4)
0(5)-0(7)	1	2.631(3)
0(6)-0(7)	1	2.622(3)
Mean		2.646
M(1) octahedron		
0(1^u)-0(2^d)	2	2.649(3)
0(1^u)-0(2^u)	2	3.204(3)
0(1^u)-0(3^d)	2	2.844(4)
0(1^u)-0(3^u)	2	3.169(4)
0(2)-0(2)	1	3.045(5)
0(2)-0(3)	2	3.091(2)
0(3)-0(3)	1	2.709(7)
Mean		2.973
M(2) octahedron		
0(1)-0(1)	1	2.621(5)
0(1^u)-0(2^d)	2	2.649(3)
0(1^u)-0(2^u)	2	2.805(3)
0(1)-0(4)	2	2.742(4)
0(2^u)-0(4^d)	2	2.811(3)
0(2^u)-0(4^u)	2	2.699(3)
0(4)-0(4)	1	2.846(5)
Mean		2.740
T(2) tetrahedron		
0(2)-0(4)	1	2.748(3)
0(2)-0(5)	1	2.664(3)
0(2)-0(6)	1	2.652(3)
0(4)-0(5)	1	2.653(3)
0(4)-0(6)	1	2.591(4)
0(5)-0(6)	1	2.680(4)
Mean		2.665
M(3) octahedron		
0(1^u)-0(1^d)	2	2.621(5)
0(1^u)-0(1^u)	2	3.378(5)
0(1^u)-0(3^d)	4	2.844(4)
0(1^u)-0(3^u)	4	3.129(4)
Mean		2.991
M(4) polyhedron		
0(2)-0(2)	1	3.045(5)
0(2^u)-0(4^d)	2	2.811(3)
0(2^u)-0(4^u)	2	3.263(3)
0(2^u)-0(5^u)	2	3.602(4)
0(4^u)-0(5^d)	2	3.359(4)
0(4^u)-0(6^u)	2	2.591(4)
0(5^u)-0(6^d)	2	3.049(3)
0(5^u)-0(6^u)	2	2.651(4)
0(6)-0(6)	1	3.369(5)
Mean		3.067

*Multiplicity

TABLE 6. SELECTED INTERATOMIC ANGLES FOR FERROGLAUCOPHANE

Atoms	*	Angle (°)
T(1) tetrahedron		
0(1)-T(1)-0(5)	1	109.5(1)
0(1)-T(1)-0(6)	1	110.3(1)
0(1)-T(1)-0(7)	1	110.0(2)
0(5)-T(1)-0(6)	1	109.9(1)
0(5)-T(1)-0(7)	1	109.0(2)
0(6)-T(1)-0(7)	1	108.1(2)
Mean		109.5
M(1) octahedron		
0(1^u)-M(1)-0(2^d)	2	78.4(1)
0(1^u)-M(1)-0(2^u)	2	99.6(1)
0(1^u)-M(1)-0(3^d)	2	84.8(1)
0(1^u)-M(1)-0(3^u)	2	97.4(1)
0(2)-M(1)-0(2)	1	92.9(1)
0(2)-M(1)-0(3)	2	94.1(1)
0(3)-M(1)-0(3)	1	79.2(1)
Mean		90.0
M(2) octahedron		
0(1)-M(2)-0(1)	1	80.4(1)
0(1^u)-M(2)-0(2^d)	2	83.4(1)
0(1^u)-M(2)-0(2^u)	2	89.6(1)
0(1)-M(2)-0(4)	2	89.8(1)
0(2^u)-M(2)-0(4^d)	2	95.4(1)
0(2^u)-M(2)-0(4^u)	2	90.5(1)
0(4)-M(2)-0(4)	1	100.6(1)
Mean		89.9
0(7)-0(7)-0(7)		67.2(2)
$^+\Delta$		0.253
T(2) tetrahedron		
0(2)-T(2)-0(4)	1	116.8(1)
0(2)-T(2)-0(5)	1	108.5(1)
0(2)-T(2)-0(6)	1	107.6(1)
0(4)-T(2)-0(5)	1	109.6(1)
0(4)-T(2)-0(6)	1	105.7(1)
0(5)-T(2)-0(6)	1	108.3(1)
Mean		109.4
M(3) octahedron		
0(1^u)-M(3)-0(1^d)	2	75.6(1)
0(1^u)-M(3)-0(1^u)	2	104.4(1)
0(1^u)-M(3)-0(3^d)	4	84.5(1)
0(1^u)-M(3)-0(3^u)	4	95.5(1)
Mean		90.0
M(4) polyhedron		
0(2)-M(4)-0(2)	1	78.6(1)
0(2^u)-M(4)-0(4^d)	2	72.8(1)
0(2^u)-M(4)-0(4^u)	2	87.1(1)
0(2^u)-M(4)-0(5^u)	2	86.6(1)
0(4^u)-M(4)-0(5^d)	2	80.6(1)
0(4^u)-M(4)-0(6^u)	2	65.5(1)
0(5^u)-M(4)-0(6^d)	2	70.0(1)
0(5^u)-M(4)-0(6^u)	2	59.7(1)
0(6)-M(4)-0(6)	1	86.5(1)
Mean		75.6
T(1)-0(5)-T(2)		134.5(2)
T(1)-0(6)-T(2)		143.9(2)
T(1)-0(7)-T(1)		148.7(3)
0(5)-0(6)-0(5)		171.2(1)
0(5)-0(7)-0(6)		170.1(2)

$^+\Delta = (90^0 - [0(7)-0(7)-0(7)])/90^0$.

*Multiplicity

TABLE 7. MAGNITUDE AND ORIENTATION OF PRINCIPAL AXES THERMAL ELLIPSOIDS FOR FERROGLAUCOPHANE

Atom	R.M.S. deviation	Angle to a-axis	Angle to b-axis	Angle to c-axis
0(1)	0.079(7)(Å)	49(17)(°)	84(18)(°)	55(19)(°)
	0.091(6)	60(24)	47(26)	129(24)
	0.101(6)	125(19)	44(26)	59(21)
0(2)	0.076(6)	93(20)	85(18)	12(22)
	0.088(6)	148(48)	122(48)	78(22)
	0.094(6)	58(48)	147(47)	92(18)
0(3)	0.097(8)	94(27)	90	10(27)
	0.102(8)	90	0	90
	0.111(8)	4(27)	90	100(27)
0(4)	0.082(7)	67(33)	23(29)	94(88)
	0.085(6)	71(39)	97(82)	171(43)
	0.110(5)	31(10)	112(10)	82(11)
0(5)	0.076(7)	113(16)	121(6)	34(10)
	0.092(6)	150(15)	94(11)	106(16)
	0.118(5)	108(9)	31(6)	61(6)
0(6)	0.071(7)	97(10)	66(6)	25(5)
	0.097(6)	155(11)	70(11)	93(11)
	0.119(5)	114(11)	148(8)	65(5)
0(7)	0.079(1)	90	0	90
	0.107(8)	119(22)	90	138(22)
	0.122(7)	151(22)	90	48(22)
T(1)	0.064(3)	91(5)	95(13)	13(7)
	0.074(3)	89(9)	175(13)	95(13)
	0.087(2)	2(7)	89(9)	102(5)
T(2)	0.066(3)	91(8)	86(15)	14(11)
	0.074(3)	112(10)	158(10)	82(16)
	0.085(2)	22(10)	111(10)	101(6)
M(1)	0.073(3)	102(4)	90	2(4)
	0.085(3)	90	0	90
	0.101(2)	12(4)	90	92(4)
M(2)	0.082(3)	88(16)	90	16(16)
	0.083(3)	90	0	90
	0.091(3)	2(16)	90	106(16)
M(3)	0.074(4)	90	0	90
	0.080(3)	90(5)	90	167(5)
	0.107(3)	0(5)	90	103(5)
M(4)	0.106(5)	130(4)	90	26(4)
	0.115(5)	90	0	90
	0.154(4)	40(4)	90	64(4)

per formula unit must occupy *M*(1) or *M*(3) or both. As the scattering factors of Mg and Al are very similar, there is no direct information available from the refinement concerning this problem. However, the ionic radii of Al^{3+} (0.53Å) and Mg^{2+} (0.72Å) differ considerably; thus, the mean bond lengths should give some indication of the site occupancies. Using the curves of Hawthorne (1978) relating mean bond-length to constituent cation and anion radii, the following calculated mean bond lengths are obtained for the two extreme distribution models:

$M(1) = 0.585Fe^{2+} + 0.348Mg + 0.067Al$
$M(3) = 0.795Fe^{2+} + 0.205Mg$
$<M(1)\text{–}O>_{calc} = 2.098Å$, $<M(1)\text{–}O>_{obs} = 2.106Å$
$<M(3)\text{-}O>_{calc} = 2.113Å$, $<\mathrm{M}(3)\text{–}O>_{obs} = 2.122Å$
$M(1) = 0.587Fe^{2+} + 0.413Mg$
$M(3) = 0.795Fe^{2+} + 0.071Mg + 0.134Al$
$<M(1)\text{–}O>_{calc} = 2.110Å$, $<M(1)\text{–}O>_{obs} = 2.106Å$
$<M(3)\text{–}O>_{calc} = 2.089Å$, $<M(3)>_{obs} = 2.122Å$

TABLE 8. SITE-OCCUPANCIES IN FERROGLAUCOPHANE

From site-population refinement:

M(1)	$0.585(6)Fe^{0} + 0.415Mg$
M(2)	$0.156(6)Fe^{0} + 0.844Al$
M(3)	$0.795(9)Fe^{0} + 0.205Mg$
M(4)	$0.860Na + 0.075Ca + 0.065Mg$

From examination of mean bond lengths:

M(1)	$0.585(6)Fe^{2+} + 0.348Mg + 0.067Al$
M(2)	$0.156(6)Fe^{3+} + 0.844Al$
M(3)	$0.795(9)Fe^{2+} + 0.205Mg$
M(4)	$0.860Na + 0.075Ca + 0.065Mg$

The root-mean-square deviations for the two extreme distributions [all Al in $M(1)$ or $M(3)$] are 0.009Å and 0.024Å, respectively, suggesting that the octahedral Al not residing in $M(2)$ is strongly ordered in the $M(1)$ position.

The refined $M(2)$ occupancy of $0.152(6)Fe^{o}$ is equal to the amount of Fe^{3+} present as indicated by the cell contents (Table 1); this factor, together with the observed mean-bond-length, suggests that all of the iron in the $M(2)$ site is Fe^{3+}. The $<M(2)\text{–}O>$ bond length and constituent $M(2)$ cation radius obtained for ferroglaucophane in this study ($<M(2)\text{–}O>$ = 1.943Å, $<r_{M(2)}>$ = 0.548Å) are fairly similar to the corresponding values obtained by Papike & Clark (1968) for glaucophane ($<M(2)\text{–}O>$ 1.943Å, $<r_{M(2)}>$ = 0.548Å) are fairly similar study, Hawthorne (1978) presented equations relating mean bond-length and constituent-cation radius for the octahedral sites in clinoamphiboles. There was some question as to the validity of the $M(2)$-site relationship at small cation radius values, and the current study was undertaken partly to resolve this point. Figure 1 shows the variation in $<M(2)\text{–}O>$ with constituent $M(2)$ cation radius. Linear regression analysis was performed, omitting the data for glaucophane and ferroglaucophane; the regression line (Table 9) is shown in Figure 1, where it can be seen that both glaucophane and ferroglaucophane deviate by ~ 0.02Å from this relationship. We may recognize two reasons for this behavior. The relationship between mean bond-length and constituent-cation radius for the $M(2)$ site may become nonlinear at small constituent-cation radii. Alternatively, the values for the mean constituent-cation radius for the points between 0.58 and 0.68Å may be wrong. The three points clustering at ~ 0.65Å (pargasite, Ti-pargasite and Kakanui hornblende, Robinson *et al.* 1973) do not have experimentally determined Fe^{3+}/Fe^{2+} ratios, and all Fe^{*} ($\equiv Fe^{2+} + Fe^{3+} + Mn$) at $M(2)$ was *assumed* to be Fe^{3+}. This means that the curve shown in Figure 1 hinges on the data point at ~ 0.59Å (ferrotschermakite, Hawthorne & Grundy 1973a). Repeating the regression analysis omitting the four data points discussed above and including the glaucophanes gives the regression line given in Table 9. The pargasite, Ti-pargasite and Kakanui hornblende data agree with this curve if some of the Fe^{*} at the $M(2)$ site is Fe^{2+}, obviously a reasonable possibility. The data point for ferrotschermakite deviates by ~ 0.015Å from this curve. It is not clear whether this minor amount of scatter at small constituent $M(2)$ cation radii reflects experimental error or a perturbation due to some other variable such as $M(4)$ cation occupancy.

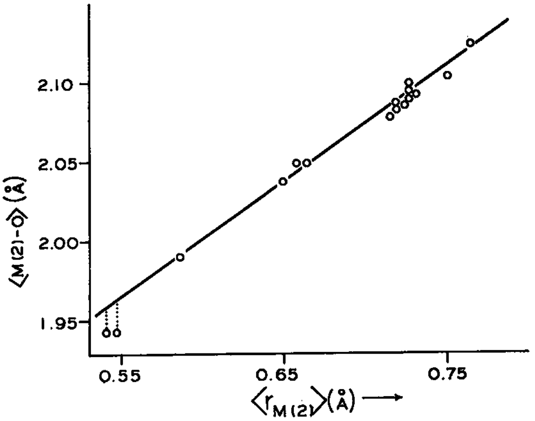

FIG. 1. Variation in $<M(2)\text{–}O>$ as a function of constituent $M(2)$ cation radius. The solid line shows the regression equation given in the text. The deviation of glaucophane and ferroglaucophane is shown by the broken lines.

The ordering of Mg/Fe^{2+} over the $M(1)$ and $M(3)$ sites observed for ferroglaucophane in this study is somewhat similar to that exhibited by glaucophane (Papike & Clark 1968); Fe^{2+} is preferentially ordered in $M(3)$. Assuming that all the Al^{VI} not resident in $M(2)$

TABLE 9. REGRESSION ANALYSIS RESULTS*

Dependent variable	Independent variable	c	m	R
1. $<M(2)\text{–}O>$	$<r_{M(2)}>$	1.585	0.694(17)	0.994
2. $<M(2)\text{–}O>$	$<r_{M(2)}>$	1.510	0.795(14)	0.998
3. $\Delta_{M(2)}$	$<Z_{M(4)}>$	2.95	1.19(12)	0.91

*Equation of the form y = mx+c

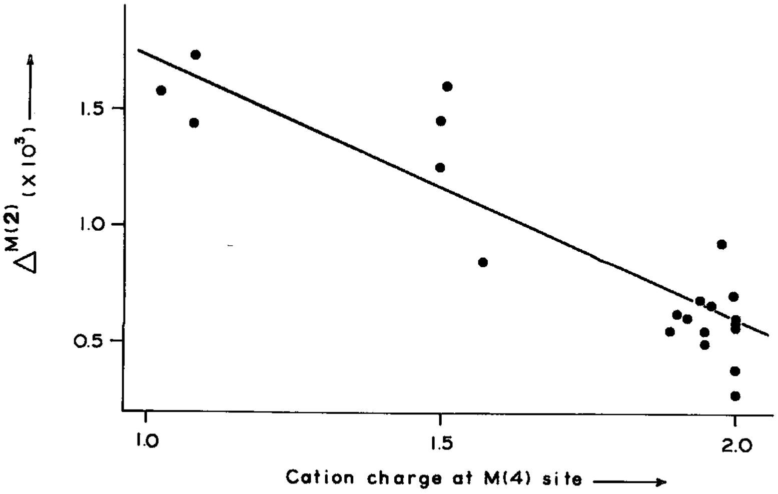

FIG. 2. Variation in bond-length distortion of $M(2)$ octahedron as a function of the mean cation charge at $M(4)$.

occurs at the $M(1)$ site, ferroglaucophane has a K_d value ($=\mathrm{Fe}^{2+}_{M(1)}\,\mathrm{Mg}_{M(3)}/\mathrm{Fe}^{2+}_{M(3)}\mathrm{Mg}_{M(1)}$) of 0.434, similar to the value of 0.466 exhibited by glaucophane.

It has been shown (Hawthorne 1978) that the bond-length distortions observed in clinoamphiboles tend to minimize the deviations from ideality in the bond-strength sums around the anions. This is of particular significance with respect to those cations coordinating the O(4) anion; all show extremely short bonds to O(4). In order to maintain mean bond-lengths in accord with the size of the constituent cations, there is a concomitant lengthening of the other bond-lengths, resulting in extremely distorted cation polyhedra. This would suggest that the variation in the bond-length distortion Δ (Brown & Shannon 1973) of the $M(2)$ octahedron in the amphiboles should be strongly affected by cations(s) occupying the $M(4)$ sites. This premise is examined in Figure 2, which shows the variation in $M(2)$ bond-length distortion as a function of the mean cation-charge (Z) at the $M(4)$ sites; a fairly good negative linear correlation is exhibited; the results of a linear regression analysis (Table 9) indicate that $\sim$ 80% of the variation in the distortion at $M(2)$ may be attributed to this factor.

AN IDEAL AMPHIBOLE STRUCTURE

Ideal models for the amphiboles were presented by Thompson (1970) and a detailed comparison of ideal topologies and observed amphibole configurations was given by Papike & Ross (1970). Both works are concerned with the space-group variations in the amphiboles and deal primarily with models involving completely rotated tetrahedral chains. The clinoamphiboles show incomplete chain rotations, which are approximated much more closely by an extended chain (*cf.*, Papike *et al.* 1973) for the analogous situation in the pyroxenes). An ideal structure may be constructed from ideal geometry analogues of the two basic repeat elements, the octahedral strip and the tetrahedral chain. These are shown in Figure 3 where the cross-linkage in the y direction is indicated by the broken lines. Crosslinkage in the x and y directions requires an octahedral: tetrahedral bond-length ratio of 4:3. Using the ionic radii of Shannon (1976), an ideal T(Si)–O bond length may be calculated; a value of 1.62Å results, in relatively good agreement with tetrahedral bond-lengths observed in amphiboles without $\mathrm{Al}^{\mathrm{IV}}$. Calculating the mean octahedral bond-length from the above ratio and subtracting the mean anion radius gives 0.78Å as the cation size necessary for complete linkage in the ideal structure; this value corresponds to [6]-coordinated Fe^{2+}.

Atomic coordinates may be derived from the ideal structure. It is convenient to work in an orthogonal coordinate system; the axes used to derive the ideal atomic coordinates of Table 10 were a^*, b and c. Comparison of these coordinates with those of the refined amphiboles (transformed to the same axial system) shows that grunerite (Finger 1969c) is the least distorted from the ideal configuration, closely followed by Mn-cummingtonite (Papike *et al.* 1969). This is in accord with the conclusion

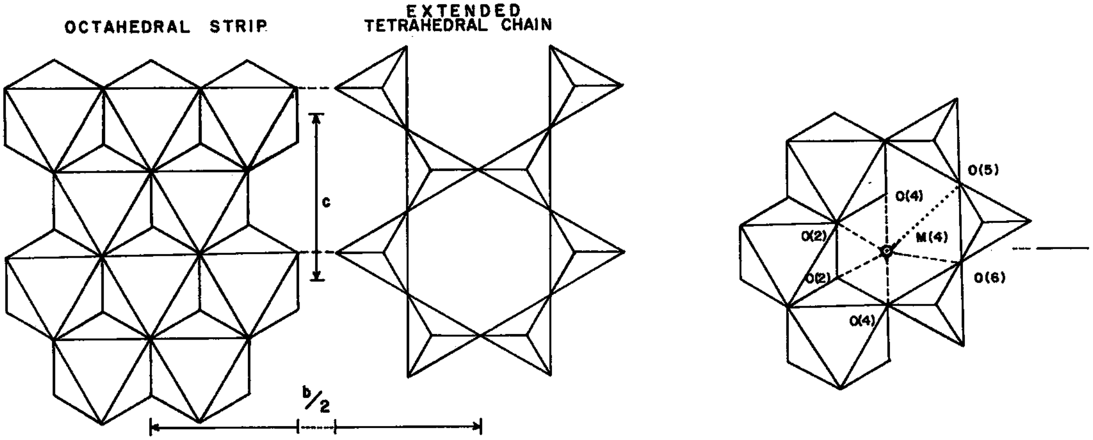

FIG. 3. Ideal polyhedral model of clinoamphibole structure involving extended chains.

TABLE 10. METRIC COORDINATES OF THE IDEAL AMPHIBOLE STRUCTURE (UPPER SET) COMPARED WITH THE METRIC COORDINATES OF GRUNERITE (LOWER SET).

Atom	x	y	z
O(1)	0.1340	0.0833	0.1667
	0.1120	0.0882	0.1631
O(2)	0.1340	0.1667	0.6667
	0.1253	0.1735	0.6679
O(3)	0.1340	0	0.6667
	0.1147	0	0.6612
O(4)	0.3660	0.2500	0.6667
	0.3839	0.2416	0.6272
O(5)	0.3660	0.1250	-0.0833
	0.3483	0.1275	-0.0767
O(6)	0.3660	0.1250	0.4167
	0.3478	0.1182	0.4246
O(7)	0.3660	0	0.1667
	0.3376	0	0.1454
T(1)	0.3080	0.0833	0.1667
	0.2867	0.0836	0.1649
T(2)	0.3080	0.1667	0.6667
	0.2993	0.1667	0.6675
M(1)	0	0.0833	1/2
	0	0.0878	1/2
M(2)	0	0.1667	0
	0	0.1794	0
M(3)	0	0	0
	0	0	0
M(4)	0	0.2500	1/2
	0	0.2574	1/2

TABLE 11. COMPARISON OF CELL DIMENSIONS IN THE IDEAL AMPHIBOLE STRUCTURE WITH THOSE OF GRUNERITE†

$$a \sin \beta = 4\sqrt{2}\,(\ell + d)/\sqrt{3}$$
$$b = 12\ell$$
$$c = 2\sqrt{3}\,\ell$$
$$\beta = \tan^{-1} 1/\sqrt{2}\,(2 + \sqrt{3})$$

	Ideal structure	Grunerite	Difference
$a \sin \beta$	9.307Å	9.358Å	0.6%
a	9.481	9.564	0.9
b	18.240	18.393	0.8
c	5.265	5.339	1.4
β	101°	101.9°	0.9
V	893.7Å^3	918.9Å^3	2.7

*2d = tetrahedral edge length for $\langle T\text{-}O \rangle$ = 1.62Å, 2ℓ = octahedral edge length.
† (Finger 1969c).

that the ideal structure can incorporate a cation the size of Fe^{2+} without any necessary distortion in order to geometrically maintain interelement linkage. Cell dimensions may be calculated for the ideal structure; these are given in Table 11 where they are compared with those of grunerite (Finger 1969c). The agreement is quite good, the mean deviation being less than 1%.

Departure of the octahedral/tetrahedral bond-length ratio from its ideal value of 4/3 must lead to some distortion of the ideal structure if interelement linkage is to be maintained. If the bond-length ratio exceeds 4/3, linkage cannot be maintained without deviation from ideal polyhedron geometry. If the bond-length ratio is less than 4/3, linkage may be maintained by a rotation (Papike & Ross 1970) of the double-chain element. If θ is the O(br)–O(br)–O(br) angle, simple geometrical arguments show that the condition

$$\langle M\text{–}O \rangle = 4/3 \, \langle T\text{–}O \rangle \sin(\theta/2)$$

is required for complete articulation. This condition also holds for cross-linkage in the y direction through sharing of the O(4) anion.

In terms of real amphibole structures, the angle θ is best calculated as the mean of all the O(br)–O(br)–O(br) angles projected onto the y–z plane. However, it is much more convenient to use just the O(5)–O(6)–O(5) angle as a measure of θ; the correlations are not particularly influenced by this approximation. Figure 4 shows the variation in tetrahedral chain

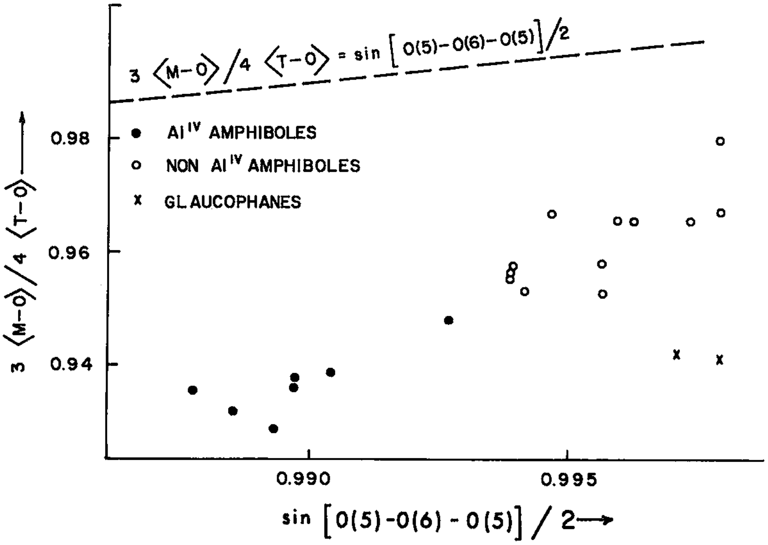

FIG. 4. Variation in $3\langle M\text{–}O\rangle/4\langle T\text{–}O\rangle$ *versus sin* [O(5)–O(6)–O(5)] /2 for *C*2/*m* clinoamphiboles. Note the deviation of the glaucophanes from the main trend of the figure.

rotation as a function of the mean octahedral/mean tetrahedral bond-length ratio; a linear correlation is very marked. It should be noted that the glaucophanes deviate significantly from the general relationship. Hawthorne & Grundy (1973b) suggested that the amount of "kinking" in the tetrahedral chain is a function of the amount of tetrahedral Al. It is apparent from the above discussion that the chemistry of the octahedral sites also significantly affects the tetrahedral-chain rotation.

Although Figure 4 shows a reasonably well-developed linear correlation, this relationship deviates significantly from equation (1). This reflects the fact that real structures are distorted from the ideal model of Figure 3, as crystal-chemical factors cause distortions from ideal polyhedron geometry that also influence the articulation requirements of the structure. Cation–cation repulsion in the octahedral strip shortens shared edges with the concomitant extension of unshared edges; thus, all octahedral edges involved in interelement linkages are increased, which will tend to compensate for the substitution of larger tetrahedral cations or smaller octahedral cations or both. Conversely, T-O(br) bonds tend to be longer than T-O(nbr) bonds, which extends the dimensions of the chain in the directions of polymerization, offsetting the cation–cation repulsion effect in the octahedral strip. Cation ordering in the sites will produce edge-sharing octahedra of disparate size, necessitating further deviation from ideal geometry. This will produce linking octahedral edges differing in length, requiring differential separation of the geminal anions of the tetrahedral chain; this feature is particularly marked for the glaucophanes and is compensated for by a marked bowing of the double chains (Papike & Clark 1968) and a tilting of the tetrahedra about the y axis such that the separation of O(1) and O(2) across O(5) is decreased and the separation of O(1) and O(2) across O(6) is increased. If this mechanism completely compensated for the difference in size of the octahedra, then the glaucophanes should not deviate from the general trend of Figure 4 as they do. However, the individual octahedra of the strip may also distort so as to promote linkage between the two basic elements. The octahedral edges involved in the linkage ($O(1^u)$–$O(2^u)$, $O(1^u)$–$O(2^u)$ and $O(1^u)$–(1^u) for $M(1)$, $M(2)$ and $M(3)$, respectively) are longer than the mean octahedral-edge length, thus promoting linkage with the tetrahedral double chain. In the non-$\mathrm{Al^{IV}}$ and low-$\mathrm{Al^{IV}}$ amphiboles, the ratio of the mean length of the linking octahedral edges to the mean octahedral edge-length is ~ 1.045 for all except the glaucophanes, whose value of ~ 1.067 is typical of the high $\mathrm{Al^{IV}}$ amphiboles. Thus, in the glaucophanes, extension of the linking octahedral edges is more important in promoting linkage than in the rest of the low $\mathrm{Al^{IV}}$ amphiboles. If the values of $3\langle M\text{-}O\rangle/4\langle T\text{-}O\rangle$ for the glaucophanes are corrected by a factor 1.067/1.045, then the values agree with the correlation shown by the rest of the amphiboles in Figure 4. Thus rotation of the tetrahedral double chain occurs to compensate for the misfit between the octahedral and tetrahedral elements of the structure.

The direction of rotation of the tetrahedral double chain (be it *O*- or *S*-rotated, Papike & Ross 1970) is irrelevant to the argument given above. It is of interest to examine the ideal structure (Fig. 3) with regard to the question of why the tetrahedral double chains are always *O*-rotated in clinoamphiboles. At the junction of the octahedral strip and the tetrahedral double chain is $M(4)$, which in the ideal structure may be sited on the 2–fold axis with the same y coordinate as the $O(4)$ anion (that is exactly on the edge of the octahedral strip); this arrangement is depicted in Figure 3. If the octahedral bond length is l, then $M(4)$–O(2) and $M(4)$–O(4) are l and $M(4)$–O(5) and $M(4)$–O(6) are $l\sqrt{42}/6$ and $l\sqrt{78}/6$, respectively. Thus, for Fe^{2+} octahedra, $l = 0.78 + 1.36 = 2.14$Å, with $M(4)$–O(5) and $M(4)$–O(6) equal to 3.15 and 2.31Å, respectively. In a $C2/m$ amphibole, *O*-rotation will shorten $M(4)$–O(5) and lengthen $M(4)$–O(6), whereas *S*-rotation will have the opposite effect. Considering the bond-strength sums around the bridging oxygens, the sum around O(6) is in excess of the ideal value of 2.0 by a much greater amount than the corresponding sum around O(5). The overall deviation from ideality will be increased by *S*-rotation and decreased by *O*-rotation of the tetrahedral chain. Thus, from this simple model, we would predict that clinoamphiboles should always show *O*-rotations. Although this seems to be the case, the model is greatly oversimplified, and the configuration of the anions surrounding the $M(4)$ sites is also affected by the tetrahedral-chain displacements (Sueno *et al.* 1973) and the bond-strength requirements of the $M(4)$ cation. The tetrahedral-chain displacement is affected by the character and amount of the tetrahedral-chain rotation and by the attitude of the O(4)–O(4) edge of the $M(2)$ octahedron. Sueno *et al.* (1973) showed that the tetrahedral-chain displacement is positively correlated with the "co-ordination coefficient" of the $M(4)$ site, which to some extent is a measure of the dispersion of the $M(4)^{\mathrm{VIII}}$–O distances. Thus, one might expect the tetrahedral chain to be *O*-rotated so as to fulfil the linkage requirements, with the O(4)–O(4) edge of the $M(2)$ octahedron adjusting to optimize the bond-strength distribution around O(5) and O(6). However, this ignores the $M(4)$ cation bond-strength requirements; even a cursory examination of Figure 3 indicates that this is an important factor. Consider first the case where $M(4) = Fe^{2+}$. The bond-strength requirements of Fe^{2+} are (approximately) satisfied by six bonds 2.14Å long; the $M(4)$ site in the ideal structure is surrounded by four atoms at 2.14Å, two atoms at 2.31Å and two atoms at 3.15Å. The O(4) anion is strongly underbonded and requires a very short $M(4)$–O(4) bond in order to satisfy its bond-strength requirements. The two $M(4)$–O(4) bonds are related by the 2–fold axis, and the only way that they may shorten from the "ideal-structure" value of 2.14Å is by moving directly towards $M(4)$. This increases the c-axis projection of the O(4)–O(4) edge of the $M(2)$ octahedron, which increases the tetrahedral-chain displacement, thus slightly shortening $M(4)$–O(6) ($\sim$ 0.01Å) and lengthening $M(4)$–O(5) ($\sim$ 0.06Å). The $M(4)$ cation (Fe^{2+}) is now overbonded and the structure compensates by a bowing of the tetrahedral double chains away from the A site and a chain rotation that has to be an *O*-rotation in order to sufficiently increase $M(4)$–O(6).

These arguments may be extended to the cases where $M(4) =$ Mn, Ca and Na; *O*-rotation of the tetrahedral chains is also necessary to achieve an adequate bond-strength distribution in this part of the structure. With the larger cations, the O(4) anions must recoil away from $M(4)$ and the cations also move away from the octahedral strip in order to achieve the longer bonds necessary for these larger cations.

ACKNOWLEDGEMENTS

The author thanks Dr. Christoph Hoffmann, Mineralogisch-Petrologisches Institut, Universität Göttingen, Germany, for providing crystals for this study, and Dr. R.B. Ferguson for his interest and encouragement. Financial support was provided by the National Research Council of Canada (grant to R.B.F.) and the University of Manitoba.

REFERENCES

BLACK, P.M. (1970): Ferroglaucophane from New Caledonia. *Amer. Mineral.* **55**, 508-511.

BOCQUET, J. (1974): Blue amphiboles of the Western Alps. Chemistry and physical characters. *Schweiz. Mineral. Petrog. Mitt.* **54**, 425-448.

BROWN, I.D. & SHANNON, R.D. (1973): Empirical bond strength — bond length curves for oxides *Acta Cryst. A* **29**, 266-282.

Coleman, R.G. (1972): Blueschist metamorphism and plate tectonics. *Int. Geol. Congr. 24th,* **2,** 19-26.

Cromer, D.T. & Liberman, D. (1970): Relativistic calculation of anomalous scattering factors for X-rays. *J. Chem. Phys.* **53,** 1891-1898.

——— & Mann, J.B. (1968): X-ray scattering factors computed from numerical Hartree-Fock wave functions. *Acta Cryst.* **A24,** 321-324.

Ernst, W. G. (1968): *Amphiboles. Crystals Chemistry, Phase Relations and Occurrence.* Springer-Verlag, New York.

——— (1971): Do mineral parageneses reflect unusually high-pressure conditions of Franciscan metamorphism? *Amer. J. Sci.* **270,** 81-108.

——— (1973): Blueschist metamorphism and P–T regimes in active subduction zones. *Tectonophys.* **17,** 255-272.

Finger, L. W. (1969a): RFINE. A Fortran IV computer program for structure factor calculation and least-squares refinement of crystal structures. *Geophys. Lab. Carnegie Inst. Wash.* (unpubl.).

——— (1969b): Determination of cation distributions by least-squares refinement of single-crystal X-ray data. *Carnegie Inst. Wash. Year Book* **67,** 216-217.

——— (1969c): The crystal structure and cation distribution of a grunerite. *Mineral. Soc. Amer. Spec. Pap.* **2,** 95-100.

Hawthorne, F. C. (1976): The crystal chemistry of the amphiboles. V. The structure and chemistry of arfvedsonite. *Can. Mineral.* **14,** 346-356.

——— (1978): The crystal chemistry of the amphiboles. VI. The stereochemistry of the octahedral strip. *Can. Mineral.* **16,** 37-52.

——— & Grundy, H.D. (1973a): The crystal chemistry of the amphiboles. I. Refinement of the crystal structure of ferrotschermakite. *Mineral. Mag.* **39,** 36-48.

——— & ——— (1973b): The crystal chemistry of the amphiboles. II. Refinement of the crystal structure of oxy-kaersutite. *Mineral. Mag.* **39,** 390-400.

——— & ——— (1976): The crystal chemistry of the amphiboles. IV. X-ray and neutron refinements of the crystal structure of tremolite. *Can. Mineral.* **14,** 334-345.

Hoffmann, C. (1970): Die Glaukophangesteine, ihre stofflichen Aquivalente und Umwandlungsprodukte in Nordcalabrien (Süditalien). *Contr. Mineral. Petrology* **27,** 283-320.

——— (1972): Natural and synthetic ferroglaucophane. *Contr. Mineral. Petrology* **34,** 135-149.

Makanjuola, A.A. & Howie, R.A. (1972): The mineralogy of the glaucophane schists and associated rocks from Ile de Groix, Brittany, France. *Contr. Mineral. Petrology* **35,** 83-118.

Papike, J.J. & Clark, J.R. (1968): The crystal structure and cation distribution of glaucophane. *Amer. Mineral.* **53,** 1156-1173.

——— & Ross, M. (1970): Gedrites: Crystal structures and intra-crystalline cation distributions. *Amer. Mineral.* **55,** 1945-1972.

———, ——— & Clark, J.R. (1969): Crystal-chemical characterization of clinoamphiboles based on five new structure refinements. *Mineral. Soc. Amer. Spec. Pap.* **2,** 117-136.

———, Prewitt, C.T., Sueno, S. & Cameron, M. (1973): Pyroxenes: comparisons of real and ideal structural topologies. *Z. Krist.* **138,** 254-273.

Robinson, K., Gibbs, G.V. & Ribbe, P.H. (1971): Quadratic elongation. A quantitative measure of distortion in coordination polyhedra. *Science* **172,** 567-570.

Shannon, R.D. (1976): Revised effective ionic radii and systematic studies of interatomic distances in halides and chalcogenides. *Acta Cryst.* **A32,** 751-757.

Sueno, S., Cameron, M., Papike, J.J. & Prewitt, C.T. (1973): The high temperature crystal chemistry of tremolite. *Amer. Mineral.* **58,** 649-664.

Thompson, J.B. Jr. (1970): Geometrical possibilities for amphibole structures: model biopyriboles. *Amer. Mineral.* **55,** 292-293 (abstr.).

Received September 1978; revised manuscript accepted November 1978.